Inorganic Chemistry

Article

Efficient Green-Blue-Light-Emitting Cationic Iridium Complex for Light-Emitting Electrochemical Cells

Md. K. Nazeeruddin,*,† R. T. Wegh,‡ Z. Zhou,‡ C. Klein,† Q. Wang,† F. De Angelis,§ S. Fantacci,§ and M. Grätzel†

Laboratory for Photonics and Interfaces, Institute of Chemical Sciences and Engineering, School of basic Sciences, Swiss Federal Institute of Technology, CH-1015 Lausanne, Switzerland, Philips Research Laboratories, High Tech Campus 4, 5656 AE Eindhoven, The Netherlands, and Istituto CNR di Scienze e Tecnologie Molecolari (ISTM-CNR), c/o Dipartimento di Chimica, Università di Perugia, I-06123 Perugia, Italy

A highly luminescent novel cationic iridium complex [iridium bis(2-phenylpyridine)(4,4′-(dimethylamino)-2,2′-bipyridine)]-PF$_6$ was synthesized and characterized using NMR, UV–visible absorption, and emission spectroscopy and electrochemical methods. This complex displays intense photoluminescence maxima in the green-blue region of the visible spectrum and exhibits unprecedented phosphorescence quantum yields, 80 ± 10% with an excited-state lifetime of 2.2 μs in a dichloromethane solution at 298 K. Single-layer light-emitting electrochemical cells with the charged complex as conducting and electroluminescent material sandwiched between indium–tin oxide and Ag electrodes were fabricated, which emit green-blue light with an onset voltage as low as 2.5 V. Density functional theory calculations were performed to provide insight into the electronic structure of the [iridium bis(2-phenylpyridine)-(4,4′-(dimethylamino)-2,2′-bipyridine)]PF$_6$ complex, comparing these results with those obtained for [iridium bis(2-phenylpyridine)(4,4′-*tert*-butyl-2,2′-bipyridine)]PF$_6$.

Introduction

Iridium(III)-cyclometalated complexes are attracting widespread interest because of their unique photophysical properties and applications in organic light-emitting diodes (OLEDs). Several groups have extensively used iridium-cyclometalated complexes in OLEDs and obtained up to 19% external quantum efficiencies, for which a multilayered structure for charge injection, transport, and light emission is required.[1-4] Another type of organic light-emitting device is the light-emitting electrochemical cell (LEC), which makes use of ionic charges to facilitate electronic charge injection from the electrodes into the organic molecular semiconductor,

eliminating the need for extra layers.[5-10] This is a promising alternative to OLED, particularly for large-area lighting applications.[10,11] Recently, Rudmann et al. have proposed a detailed operating mechanism for a LEC based on transition-metal complexes.[12]

The possible operating mechanism of a LEC is schematically shown in Figure 1. Upon application of a bias, the cations and anions present in the organic layer move toward the cathode and anode, respectively, leading to large electric

* To whom correspondence should be addressed. E-mail: MdKhaja.Nazeeruddin@epfl.ch.
† Swiss Federal Institute of Technology.
‡ Philips Research Laboratories.
§ Università di Perugia.

(1) Adachi, C.; Baldo, M. A.; Thompson, M. E.; Forrest, S. R. *J. Appl. Phys.* **2001**, *90*, 5048.
(2) Baldo, M. A.; Lamansky, S.; Burrows, P. E.; Thompson, M. E.; Forrest, S. R. *Appl. Phys. Lett.* **1999**, *75*, 4.
(3) Ikai, M.; Tokito, S.; Sakamoto, Y.; Suzuki, T.; Taga, Y. *Appl. Phys. Lett.* **2001**, *79*, 156.
(4) Nazeeruddin, M. K.; Humphry-Baker, R.; Berner, D.; Rivier, B. S.; Zuppiroli, L.; Grätzel, M. *J. Am. Chem. Soc.* **2003**, *125*, 8790−8797.

(5) Pei, Q.; Yu, G.; Zhang, C.; Yang, Y.; Heeger, A. J. *Science* **1995**, *269*, 1086.
(6) Slinker, J. D.; Gorodetsky, A. A.; Lowry, M. S.; Wang, J.; Parker, S.; Rohl, R.; Bernhard, S.; Malliaras, G. G. *J. Am. Chem. Soc.* **2004**, *126*, 2763.
(7) Slinker, J.; Bernards, D.; Houston, P. L.; Abruna, H. D.; Bernhard, S.; Malliaras, G. G. *Chem. Commun.* **2003**, 2392.
(8) Rudmann, H.; Shimida, S.; Rubner, M. F. *J. Am. Chem. Soc.* **2002**, *124*, 4918.
(9) Bernhard, S.; Barron, J. A.; Houston, P. L.; Abruna, H. D.; Ruglovksy, J. L.; Gao, X.; Malliaras, G. G. *J. Am. Chem. Soc.* **2002**, *124*, 13624.
(10) Wegh, R. T.; Meijer, E. J.; Plummer, E. A.; De Cola, L.; Brunner, K.; van Dijken, A.; Hofstraat, J. W. *Proc. SPIE* **2004**, *5519*, 48−58.
(11) Tmayo, A. B.; Garon, S.; Sajoto, T.; Djurovich, P. I.; Tsyba, I. M.; Bau, R.; Thompson, M. E. *Inorg. Chem.* **2005**, *44*, 8723−8732.
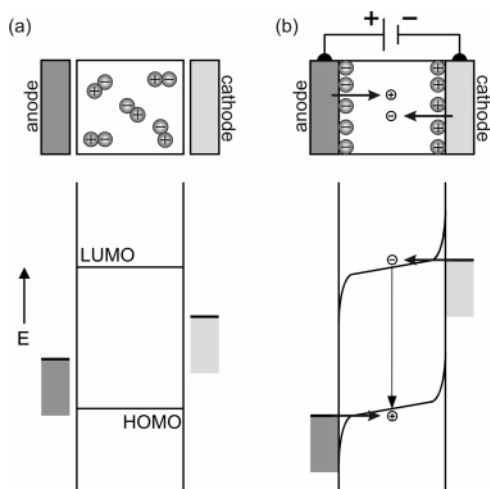(12) Rudmann, H.; Shimada, S.; Rubner, M. F. *J. Appl. Phys.* **2003**, *94*, 115.

Figure 1. Operating mechanism of a LEC. The top pictures are cross sections, and the bottom pictures are energy band diagrams. (a) Relative positions of the energy levels when the layers are not in contact: the Fermi levels of the electrodes are not matched with the HOMO and LUMO levels of the electroluminescent layer. The ions in that layer reside in pairs. (b) Situation when a voltage is applied high enough to overcome the HOMO−LUMO gap of the electroluminescent layer ($V \geq E_g/e$). The ionic double layers built up at the electrode interfaces enable electronic charge carrier injection, which after recombination leads to emission of a photon.

fields at the electrode interfaces. The ion distribution formed facilitates injection of electrons and holes at the cathode and anode, respectively, which after transport and recombination of the charge carriers can result in emission of a photon. As can be seen in Figure 1, the ionic charges enable charge injection at a bias just exceeding the potential to overcome the highest occupied molecular orbital (HOMO)−lowest unoccupied molecular orbital (LUMO) gap of the electroluminescent material (i.e., $V \geq E_g/e$), irrespective of the energy levels of the electrodes. This mechanism leads to three advantages of LECs with respect to OLEDs:[10] first, stable metals such as aluminum, silver, or gold can be used as the cathode; second, thicker organic active layers can be used while keeping the operating voltage low, thus preventing the occurrence of shorts; and third, no additional layers for charge injection are needed, keeping the device structure simple. These advantages of LECs open the road to possibly nonencapsulated stable large-area devices, which is particularly attractive for lighting applications.

The majority of ionic complexes that were used in these types of single-layer devices have been ruthenium complexes, which emit in the 600−650-nm region.[7−9,13,14] For lighting applications, white light is needed, which can be obtained by mixing blue with one or more other colors. Thus, the design and development of highly phosphorescent blue-emitting charged iridium complexes are desired.[4,15−17] Slinker et al. have used fluorinated 2-phenylpyridine ligands to obtain

iridium cationic complexes that show green-blue[17] and green[18] electroluminescence. In these complexes, the increase in the HOMO−LUMO gap with respect to complexes without fluorine substitution was due to stabilization of the HOMO.[17] Recently, Thomson et al. have used an interesting approach to obtain blue electroluminescence by stabilizing the HOMO of iridium cationic complexes using a 1-phenylpyrazole ligand.[11] Here we demonstrate the ability to tune the emission color of a highly phosphorescent cationic iridium complex from yellow to blue by meticulous selection of a dimethylamino-substituted bipyridine donor ligand. As will be shown, in this case the HOMO−LUMO gap is increased because of a larger destabilization of the LUMO than of the HOMO.

Experimental Section

Materials and Measurements. All of the solvents and chemicals, unless stated otherwise, were purchased from Fluka, puriss grade. UV−visible and fluorescence spectra were recorded in a 1-cm-path-length quartz cell on a Cary 5 spectrophotometer and a Spex Fluorolog 112 spectrofluorimeter, respectively. Electrochemical data were obtained by using a PC-controlled AutoLab PSTAT10 electrochemical workstation (Eco Chimie), in which a platinum disk working electrode, a platinum coil auxiliary electrode, and a silver disk quasi-reference electrode were mounted in a single-compartment-cell configuration. ^{1}H and ^{13}C NMR spectra were measured on a Bruker 200-MHz spectrometer. The reported chemical shifts were in ppm versus tetramethylsilane.

The quantum yields were determined using the following equation:[19,20]

$$\phi_X = \phi r K_{opt} \frac{(D/A_{exc})_X}{(D/A_{exc})_r}$$

where the subscripts X denote the substance whose quantum yield is determined and r is the reference substance quinine sulfate (3×10^{-5} M in 1 M H$_2$SO$_4$), whose luminescence quantum yield is known to be 0.545;[20] K_{opt} is the optical factor referring to the higher refractive index of dichloromethane ($n_D = 1.424$) compared to the water solution ($n_D = 1.333$); D is the integrated area under the emission spectrum; and A_{exc} is the absorbance at the exciting wavelength.

LEC. The iridium complex [iridium bis(2-phenylpyridine)(4,4′-(dimethylamino)-2,2′-bipyridine)]PF$_6$ was dissolved in acetonitrile (20 mg/mL) by stirring at 50 °C for 30 min. The solution was brought into a nitrogen-atmosphere glovebox, where all subsequent processing was carried out. Molecular sieves were added in order to remove traces of water. After 30 min, the solution was filtrated and spin-coated on glass substrates with structured indium−tin oxide (ITO), which had been thoroughly cleaned beforehand using soap, water, 2-propanol, ultrasound, and UV ozone. This resulted in homogeneous films of nearly 100-nm thickness. The films were dried at 100 °C in nitrogen for about $^1/_2$ h. A 100-nm-thick silver electrode was evaporated on top in a vacuum chamber at a rate of 0.5 nm/s.[10]

Synthesis of [Iridium bis(2-phenylpyridine)(4,4′-(dimethylamino)-2,2′-bipyridine)]PF$_6$. The dimeric iridium(III) complex

(13) Handy, E. S.; Pal, A. J.; Rubner, M. F. *J. Am. Chem. Soc.* **1999**, *121*, 3525.
(14) Gao, F. G.; Bard, A. J. *J. Am. Chem. Soc.* **2000**, *122*, 7426.
(15) Coppo, P.; Plummer, E. A.; De Cola, L. *Chem. Commun.* **2004**, 1774−1775.
(16) Lowry, M. S.; Hudson, W. R.; Pascal, R. A. J.; Bernhard, S. *J. Am. Chem. Soc.* **2004**, *126*, 14129.
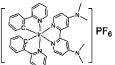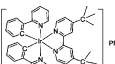(17) Lowry, M. S.; Goldsmith, J. I.; Slinker, J. D.; Rohl, R.; Pascal, R. A.; Malliaras, G. G.; Bernhard, S. *Chem. Mater.* **2005**, *17*, 5712.

(18) Slinker, J. D.; Koh, C. Y.; Malliaras, G. G.; Lowry, M. S.; Bernhard, S. *Appl. Phys. Lett.* **2005**, *86*, 173506.
(19) Parker, C. A. *Measurement of Fluorescence Efficiency*; Elsevier Publishing Co.: New York, 1968.
(20) Kartens, T.; Kobs, K. *J. Phys. Chem.* **1980**, *84*, 1871.

Table 1. Absorption, Emission, and Electrochemical Properties of the Iridium Cationic Complexes N926 and [Ir(ppy)$_2$(dtb-bpy)]PF$_6$

Complex	Absorption, λ_{max} (nm)	Emission λ_{max} (nm)	Electrochemical data V vs. Fc[c]		Em. ϕ[d]	Lifetime τ (µs)[d]
			$E^{1/2}$ oxidation	$E^{1/2}$ reduction		
N926	268; 290; 356; 376; 444[a]	491, 520[b]	0.72	-2.17 -2.61 -2.87	0.8 ± 0.1	2.2±0.02 (0.63)
[e]	not given	581	0.83	-1.88[e]	0.235	0.557

[a] Absorption data were measured in a CH$_2$Cl$_2$ solution. [b] Emission data were collected at 298 K by excitation at 380 nm. [c] Electrochemical measurements were carried out in an acetonitrile solution, and the potentials are in volts vs ferrocinium/ferrocene (Fc). [d] Quantum yield and liftetime data are collected in deaerated solutions; the value in parentheses is in an aerated solution. [e] Data taken from ref 6.

[Ir(ppy)$_2$(Cl)]$_2$ (300 mg, 0.28 mM) was dissolved in 100 mL of a dichloromethane solvent under nitrogen. To this solution was added a 4,4′-(dimethylamino)-2,2′-bipyridine ligand[21,22] (176 mg, 0.724 mM). The reaction mixture was refluxed under nitrogen for 3 h. The solvent dichloromethane was[20] evaporated, and the resulting solid was dissolved in 5 mL of methanol. Then, by the addition of a hexafluorophosphate salt solution in methanol, [iridium bis(2-phenylpyridine)(4,4′-(dimethylamino)-2,2′-bipyridine)]PF$_6$ was precipitated. Yield: 306 mg, 50%.

^{1}H NMR (CD$_3$OD): δ 8.14 (2H, d, *J* = 8 Hz), 7.88 (4H, d, *J* = 8 Hz), 7.79 (2H, t, *J* = 6 Hz), 7.79 (2H, s), 7.69 (2H, d, *J* = 7.6 Hz), 7.47 (2H, dd, *J* = 6 and 2 Hz), 7.10 (2H, t, *J* = 6.6 Hz), 7.04 (2H, t, *J* = 7.6 Hz), 6.68 (2H, dd, *J* = 6.6 Hz), 6.35 (2H, dd, *J* = 7.5 Hz). ^{13}C NMR (CD$_2$Cl$_2$): δ 166.96, 156.7, 155.53, 153.18, 149.79, 149.31, 144.73, 136.19, 132.59, 131.08, 125.41, 123.47, 122.60, 120.09, 110.04, 105.97. Anal. Calcd for C$_{36}$H$_{34}$F$_6$IrN$_6$P: C, 48.70; H, 3.86; N, 9.47. Found: C, 48.69; H, 4.01; N, 9.84.

Results and Discussion

The mixed-ligand complex [iridium bis(2-phenylpyridine)-(4,4′-(dimethylamino)-2,2′-bipyridine)]PF$_6$ (see Table 1 for the chemical structure; further called N926) was synthesized in dichloromethane starting from the dichloro-bridged iridium(III) dimer [Ir$_2$(2-phenylpyridine)$_4$(Cl$_2$)] and 4,4′-(dimethylamino)-2,2′-bipyridine,[21,22] yielding a yellow powder. The ^{1}H NMR spectrum shows 11 different proton resonances, out of which eight are due to the 2-phenylpyridine ligands and the remaining three are due to 4,4′-(dimethylamino)-2,2′-bipyridine protons. The ^{13}C NMR spectrum shows 16 peaks, consistent with the complex (see synthesis section).

The cyclic voltammogram of the complex (Figure 2) measured in acetonitrile containing 0.1 M tetrabutylammonium hexafluorophosphate with a 100 mV/s scan rate shows a reversible oxidation wave at 0.72 V vs Fc due to oxidation of iridium(III) to iridium(IV). Compared to the previously reported [iridium bis(2-phenylpyridine)(4,4′-*tert*-butyl-2,2′-bipyridine)]PF$_6$ complex (see Table 1; further called [Ir(ppy)$_2$-(dtb-bpy)]PF$_6$),[6] the N926 oxidation wave is cathodically shifted by 110 mV because of the donor strength of 4,4′-(dimethylamino)-2,2′-bipyridine (i.e., the HOMO is desta-

(21) Zakeeruddin, S. M.; Fraser, D. M.; Nazeeruddin, M. K.; Graetzel, M. *J. Electroanal. Chem.* **1992**, *337*, 253–283.
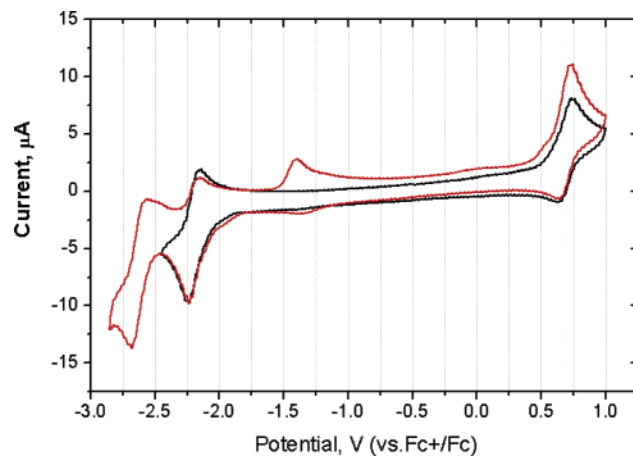(22) Maerker, G.; Case, F. H. *J. Am. Chem. Soc.* **1958**, *80*, 2745.

Figure 2. Cyclic voltammogram of N926 measured in acetonitrile in the presence of 0.1 M tetrabutylammonium hexafluorophosphate as the supporting electrolyte with a 100 mV/s scan speed. The black line shows scanning between −2.4 to +1 V and the red line between −2.8 and +1 V. The observed irreversible new wave at around −1.35 V is due to an unknown product that is formed when scanning beyond −2.4 V.
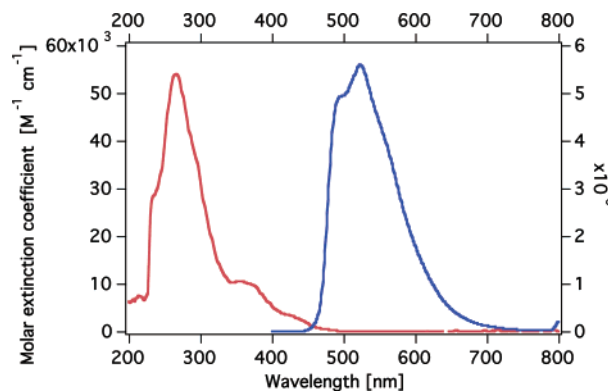

Figure 3. Absorption and emission spectra of N926 in a dichloromethane solution (concentration 5 × 10^{-6} M) at 298 K. The excitation wavelength for the emission spectrum was 380 nm.

bilized by 110 mV). The three reversible reduction waves at −2.17, −2.61, and −2.87 V vs Fc (only two waves are shown in Figure 2) are assigned to the reduction of 4,4′-(dimethylamino)-2,2′-bipyridine and the two 2-phenylpyridine ligands, respectively (Table 1). It is interesting to note that the ligand-based reduction potential, which corresponds to the LUMO (first reduction couple), is significantly shifted cathodically (290 mV) compared to [Ir(ppy)$_2$(dtb-bpy)]PF$_6$.[6] This demonstrates that the destabilization of the ligand-based LUMO orbitals more than offsets the destabilization of the metal-based HOMO orbitals, both caused by the donor ligand 4,4′-(dimethylamino)-2,2′-bipyridine, ensuring an increase in the gap between the HOMO and LUMO of N926 compared to the HOMO and LUMO of [Ir(ppy)$_2$(dtb-bpy)]PF$_6$.

Figure 3 shows absorption and emission spectra of the cationic N926 complex measured in a dichloromethane solution at 298 K. The absorption spectrum displays bands in the UV at 268, 290, 356, and 376 nm and in the visible region at 444 nm due to intraligand (π−π^*) and metal-to-ligand charge-transfer transitions (MLCTs), respectively (Figure 3).[23] The N926 complex, when excited within the

(23) Schmid, B.; Garces, F. O.; Watts, R. J. *Inorg. Chem.* **1994**, *33*, 9.

$\pi-\pi*$ and MLCT absorption bands at 298 K, shows emission maxima at 490 and 520 nm, with 2.2-μs lifetimes. This is a clear blue shift of around 60 nm compared to the parent [iridium bis(2-phenylpyridine)(4,4′-*tert*-butyl-2,2′-bipyridine)]PF$_6$ and [iridium bis(2-phenylpyridine)(2,2′-bipyridine)]PF$_6$ complexes.[6,24] The emission maximum is in the same range as that for a solution of the fluorinated complex [Ir(dF(CF$_3$)ppy)$_2$(dtb-ppy)]PF$_6$.[17] It is worth noting that the argon-deaerated dichloromethane solution of N926 shows bright luminescence under a UV lamp in a lighted room and displays an unusual phosphorescence quantum yield of 80 ± 10% in a solution at room temperature. The emission spectral profile is independent of the excitation wavelength and the emission decayed as a single exponential with a lifetime of 2.2 μs in a degassed CH$_2$Cl$_2$ solution, which is indicative of strong spin−orbit coupling leading to intersystem crossing from the singlet to the triplet states.[25]

Orthometalated iridium complexes are known to have the highest triplet emission quantum yields because of several factors:[26,27] (a) Iridium has a large ligand-field splitting of the d orbital compared to other metals in the series. (b) The ligand-field strength of the phenylpyridine anionic ligand is strong, increasing the d-orbital splitting even further, leading to an enlarged gap between the e$_g$ orbitals of iridium and the LUMO of the ligand. (c) $\pi-\pi*$ and MLCT transitions are close-lying, which together with the heavy-atom effect enhances the spin−orbit coupling. However, generally the mixed-ligand cationic iridium complexes show appreciably lower quantum yields compared to the tris-orthometalated iridium complexes because of the lower LUMO orbitals of the 2,2′-bipyridine ligand.[6,24,28] One strategy to increase the band gap and the quantum yields of iridium complexes is to introduce fluorine and/or CF$_3$ substituents. This results in a stabilization of both the HOMO and LUMO, and because the HOMO stabilization is larger, this leads to an increased gap.[17] The strategy we have chosen, however, is to decrease the gap between the lowest $\pi*$ orbitals of the 2-phenylpyridine and 2,2′-bipyridine ligands by introducing donor substituents such as dimethylamino groups at the 4,4′ positions of 2,2′-bipyridine, which are known to have a strong destabilization effect on the LUMO. In such types of complexes, the $\pi-\pi*$ and MLCT states associated with the 2-phenylpyridine and 4,4′-(dimethylamino)-2,2′-bipyridine ligands are expected to be located closely together, which enhances the excited-state decay through radiative pathways.

The quantum yield of N926 was measured using recrystallized quinine sulfate in 1 N H$_2$SO$_4$ as a quantum yield standard. In addition, the widely referred to complex Ru-(bpy)$_3$(PF$_6$)$_2$ was used as a secondary standard to verify the yields obtained with quinine sulfate. The data obtained using both standards are in excellent agreement and indeed show

remarkably high yields, i.e., 80%. Therefore, this class of compounds provides an exciting opportunity to enhance the quantum yields and to tune the emission spectral properties from yellow to blue by simply selecting appropriate donor ligands.

To provide insight into the electronic structure of the N926 complex, we performed density functional theory (DFT) calculations on both N926 and [iridium bis(2-phenylpyridine)(4,4′-*tert*-butyl-2,2′-bipyridine)]$^+$. The geometries of the two cationic complexes were optimized using the BP86 exchange-correlation function,[29] together with a TZP (DZP) basis set for iridium (N, C, H), including scalar-relativistic corrections as implemented in the *ADF* program.[30] All of the calculations reported in this paper have been performed within C$_2$ any symmetry constraints to capture the possible deviations from ideal O_h symmetry exhibited by the investigated complexes. Nevertheless, we refer to the highest occupied metal-based MOs as t$_{2g}$, using O_h symmetry labels for clarity. The calculated geometrical parameters are in excellent agreement with experimental data for the related complex [iridium bis(2-phenylpyridine)(4,4′-C$_9$H$_{19}$-2,2′-bipyridine)]$^+$, for which X-ray data are available.[31] Ir−N and Ir−C distances of 2.162 (bpy), 2.052 (ppy), and 2.007 Å are calculated, to be compared to experimental values of 2.151, 2.057, and 2.015 Å, respectively. Bond angles are also accurately reproduced.

On the optimized geometries, we performed single-point calculations at the B3LYP/LANL2DZ level of theory[32,33] in an acetonitrile solution by means of the PCM solvation model,[34] as implemented in the *Gaussian03* program package.[35] The results are reported in Figure 4, together with plots of selected MOs.

The HOMO of both complexes is an antibonding combination of Ir(t$_{2g}$) and ppy(π) orbitals (see Figure 4) and is calculated at −5.50 and −5.66 eV for N926 and [Ir(ppy)$_2$-(dtb-bpy)]$^+$, respectively. For N926, the HOMO is followed, in order of decreasing energy, by two combinations of Ir-(t$_{2g}$) and N lone pairs of the 4,4′-(dimethylamino)-2,2′-bipyridine ligand, which are missing in the [Ir(ppy)$_2$(dtb-bpy)]$^+$ complex. At still lower energy, five combinations of Ir(t$_{2g}$) and ppy(π), with variable percentage of metal character, are found, which are followed by the π-bonding framework of the 4,4′-(dimethylamino)-2,2′-bipyridine ligand. The LUMO of both complexes is a $\pi*$ orbital localized on the 4,4′-substituted bipyridine ligand and is calculated at −2.03 and −2.49 eV for N926 and [Ir(ppy)$_2$(dtb-bpy)]$^+$, respectively. At higher energy, the LUMO is followed by an almost degenerate couple of phenylpyridine $\pi*$ orbitals.

(24) King, K. A.; Watts, R. J. *J. Am. Chem. Soc.* **1987**, *109*, 1589−1590.
(25) Ichimura, K.; Kobayashi, T.; King, K. A.; Watts, R. J. *J. Phys. Chem.* **1987**, *91*, 6104.
(26) Ohsawa, Y.; Sprouse, S.; King, K. A.; DeArmond, M. K.; Hanck, K. W.; Watts, R. J. *J. Phys. Chem.* **1987**, *91*, 1047.
(27) Garces, F. O.; King, K. A.; Watts, R. J. *Inorg. Chem.* **1988**, *27*, 3464.
(28) Yang, C.-H.; Li, S.-W.; Chi, Y.; Cheng, Y.-M.; Yeh, Y.-S.; Chou, P.-T.; Lee, G.-H. *Inorg. Chem.* **2005**, *44*, 7770−7780.

(29) Becke, A. D. *Phys. Rev. A* **1988**, *38*, 3098.
(30) te Velde, G.; Bickelhaupt, F. M.; Baerends, E. J.; Fonseca-Guerra, C.; van Gisbergen, S. J. A.; Snijders, J. G.; Ziegler, T. *J. Comput. Chem.* **2001**, *22*, 931.
(31) Neve, F.; La Deda, M.; Crispini, A.; Bellusci, A.; Puntoriero, F.; Campagna, S. *Organometallics* **2004**, *23*, 5856.
(32) Becke, A. D. *J. Chem. Phys.* **1993**, *98*, 5648−5652.
(33) Hay, P. J.; Wadt, W. R. *J. Chem. Phys.* **1985**, *82*, 270.
(34) Miertus, S.; Scrocco, S.; Tomasi, T. *Chem. Phys.* **1981**, *55*, 117.
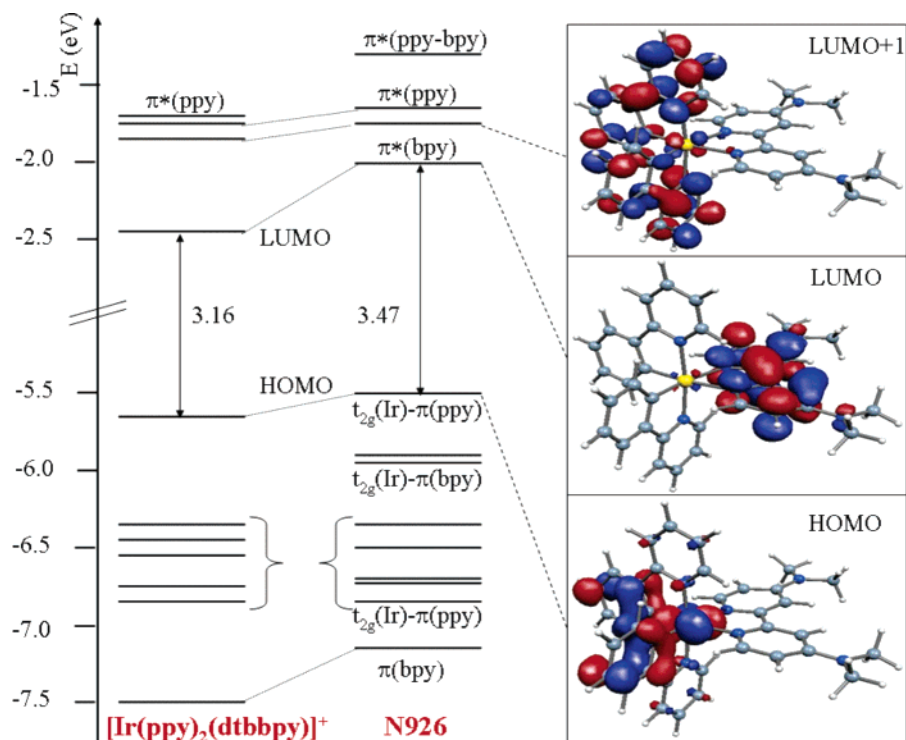(35) Frisch, M. J. *Gaussian03*, revision B.05; Gaussian, Inc.: Wallingford, CT, 2004.

Figure 4. Energy and character of the frontier MOs of N926 and [Ir(ppy)₂(dtb-bpy)]⁺. Also shown are isodensity plots of selected MOs.

Our calculated electronic structure is consistent with experimental electrochemical data, which showed cathodic shifts of the oxidation and reduction potentials of 110 and 290 mV, respectively, on going from [Ir(ppy)₂(dtb-bpy)]⁺ to the N926 complex. Indeed, HOMO and LUMO energy upshifts of 0.16 and 0.47 eV are computed for the N926 complex, as a result of the different destabilization of the HOMO and LUMO, which translates into an increase of the HOMO−LUMO gap from 3.16 to 3.47 eV. This is the result of the increased charge donation of 4,4′-dimethylamino with respect to 4,4′-*tert*-butyl groups attached to the 2,2′-bipyridine ligand, which induces a larger energy shift on the ligand-based LUMO than on the metal-based HOMO. There is some discrepancy in absolute value with the experimental electrochemical band gap (2.89 V for N926), but a similar difference was found in comparable calculations on a fluorinated cationic iridium complex.[17] In any case, the DFT calculation clearly confirms and explains the trend in energy level shifts for the different substituents.

To investigate the electroluminescence properties of the [iridium bis(2-phenylpyridine)(4,4′-(dimethylamino)-2,2′-bipyridine)]PF₆ complex, LECs were fabricated in a nitrogen-atmosphere glovebox.[10] They consisted of a 100-nm spin-coated layer of pristine N926 sandwiched between an ITO and an evaporated silver electrode (for more details, see the Experimental section).

It is well-known that solid-state LECs exhibit a significant response time because electroluminescence can only occur after the ionic double layers have been built up at the electrode interfaces.[7,10] Because in this case only the PF₆⁻ anion is mobile, the double layers are formed by accumulation and depletion of PF₆⁻ at the anode and cathode, respectively. For the present device, upon application of a
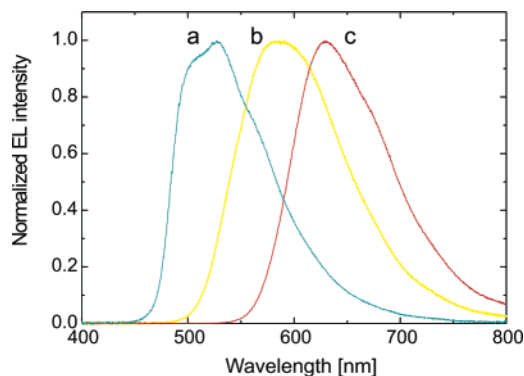

Figure 5. Electroluminescence spectra of ITO/electroluminescence (EL) layer/Ag devices, where the EL layer consists of [Ir(ppy)₂(dma-bpy)]PF₆ (a), [Ir(ppy)₂(bpy)]PF₆ + PMMA (b), and [Ru(bpy)₃](PF₆)₂ + PMMA (c). The EL intensities are in arbitrary units.

bias of 5 V, it started to emit green-blue light after several minutes. The electroluminescence spectrum, as shown in Figure 5 (trace a), is similar to the photoluminescence spectrum recorded for a spin-coated film on glass and of a solution of the complex (Figure 3), in contrast to [Ir(dF-(CF₃)ppy)₂(dtb-ppy)] PF₆.[17] For comparison, the electroluminescence spectra recorded for similar devices with [Ir(ppy)₂(bpy)]PF₆ (trace b, yellow emission) and [Ru(bpy)₃](PF₆)₂ (trace c, orange-red emission) as the active material are also shown.[10]

To investigate the performance of the device as a function of the applied bias in a steady-state situation, the measurement as shown in Figure 6a was performed.[10] First, the LEC was precharged at 5 V until stable values for current, light, and voltage were reached (in this case that means that first the current density increased until the compliance set at 0.44 mA/mm² was reached, after which the current remained
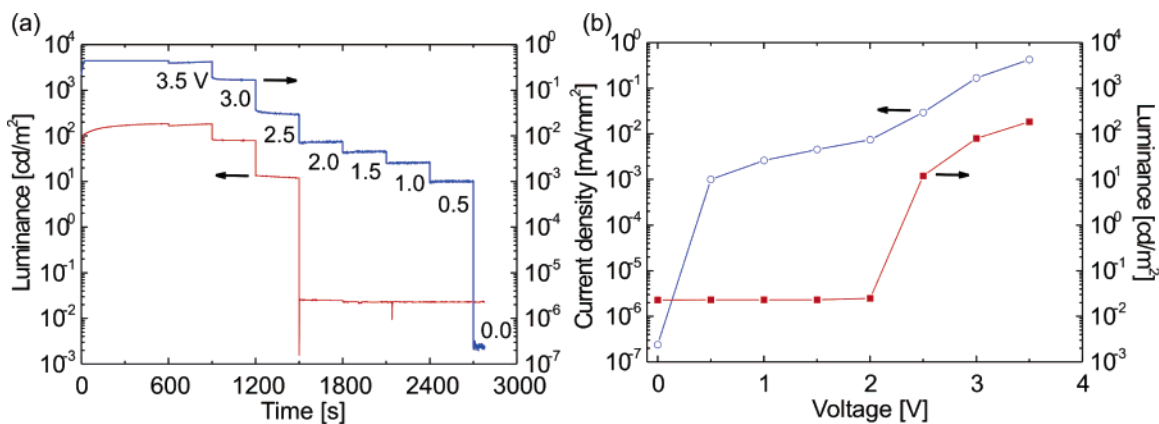
Figure 6. (a) Current density (blue trace) and photocurrent (red trace) vs time for an ITO/[Ir(ppy)$_2$(dma-bpy)]PF$_6$/Ag LEC. The numbers in the graph area denote the voltages applied. Before the start of this measurement, the device was precharged at 5 V. (b) Steady-state current density (circles) and photocurrent (squares) vs voltage, as derived from part a. The traces are guides to the eye.

constant and the voltage decreased to a stable value of about 3.5 V). Subsequently, the bias was decreased in steps of 0.5 V, and at every step, the current and light were monitored for 300 s. At the end of each bias step, steady state was reached, and these equilibrium values for the current and photocurrent are plotted against the voltage in Figure 6b. The behavior is comparable to what we observed for devices based on [Ru(bpy)$_3$](PF$_6$)$_2$ and [Ir(ppy)$_2$(bpy)]PF$_6$.[10] Upon a decrease in the bias, the light output and current density first decrease correspondingly. Between 2.0 and 0.5 V, no light is emitted, but a significant current density is found and can be attributed to leakage.[10] The onset voltage for light emission is around 2−2.5 V, which is very low regarding the electrochemical HOMO−LUMO gap found to be 2.97 V. We have observed sub-bandgap electroluminescence also for devices based on [Ru(bpy)$_3$](PF$_6$)$_2$, and it has been explained by thermal excitation of charge carriers.[36] The fact that green-blue emission is obtained with a silver cathode at a voltage as low as 2.5 V shows the advantage of using a LEC.

The LEC device showed a luminescence of around 200 cd/m^2 at 3.5 V, leading to an efficacy on the order of 0.43 cd/A, corresponding to an equivalent quantum efficiency of around 0.2%. The light output is not very high as a result of concentration quenching because the iridium complex is the sole component of the active layer. When the complex is mixed with a suitable host, the light output and efficiency will be significantly higher.

In conclusion, we have synthesized a novel green-blue phosphorescent cationic complex, [iridium bis(2-phenylpyridine)(4,4′-(dimethylamino)-2,2′-bipyridine)]PF$_6$, by engineering at the molecular level. It exhibits photoluminescence quantum yields of 80 ± 10%, due to close-lying LUMO orbitals of 2-phenylpyridine and 4,4′-(dimethylamino)-2,2′-bipyridine. The LEC device based on the new complex emits green-blue light at a bias as low as 2.5 V. This study demonstrates the significance of simple design principles leading to desired properties for practical applications. Also, it is conceivable to develop deep-blue electroluminescent cationic complexes by using fluorinated 2-phenylpyridine or 1-phenylpyrazole ligands that stabilize the HOMO orbitals and dimethylamino-substituted bipyridine ligands that destabilize the LUMO orbitals, resulting in a significantly increased gap between the HOMO and LUMO. The work directed toward this goal is in progress in our laboratory.

(36) De Mello, J. C.; Tessler, N.; Graham, S. C.; Friend, R. H. *Phys. Rev. B* **1998**, *57*, 12951.